

Seasonal patterns and diagnostic values of $\delta^2\text{H}$, $\delta^{18}\text{O}$, d-excess, and $\Delta^{17}\text{O}$ in precipitation over Seoul, South Korea (2016–2020)

Songyi Kim^{1,2}, Yeongcheol Han², Hyejung Jung¹, Jeonghoon Lee¹

5 ¹Department of Science Education, Ewha Womans University, Seoul, 03760, Republic of Korea

²Division of Glacier & Earth Sciences, Incheon, 21190, Korea Polar Research Institute, Republic of Korea

Correspondence to: Jeonghoon Lee (jeonghoon.d.lee@gmail.com)

Abstract. Precipitation stable isotopes are critical tracers for understanding climate variability and the hydrological cycle, as they enable the tracing of moisture sources, air mass mixing, and evaporation–condensation mechanisms. In mid-latitude regions such as South Korea, which are influenced by tropical and extratropical circulation, long-term isotope records remain scarce. Here, we analyze stable isotopes in precipitation collected bi-weekly in Seoul, South Korea, from 2016 to 2020. The oxygen isotope composition ($\delta^{18}\text{O}$) ranged widely from 1.15 to -18.21‰ , hydrogen isotope composition ($\delta^2\text{H}$) varied from 3.3 to -132.0‰ , and the ^{17}O -excess ($\Delta^{17}\text{O}$) ranged from 69 to -28‰ . All three primary isotopes exhibited a coherent sinusoidal seasonal cycle, with the most depleted values in winter, gradual enrichment through spring, and sharp depletion during the summer monsoon, reflecting the combined influence of temperature and the amount effect. The deuterium excess (d-excess) was highest during cold, dry months and lowest in humid, rainy months, reflecting shifts in relative humidity and kinetic fractionation. Meanwhile, $\Delta^{17}\text{O}$ exhibited a similar season trend with a smaller amplitude, suggesting that, beyond its known dependence on relative humidity and kinetic fractionation, it is also modulated by large-scale transport and vapor mixing. The local meteoric water line closely matches the global line but winter samples show a higher intercept and a slightly steeper $\delta^{17}\text{O}$ – $\delta^{18}\text{O}$ slope, suggesting enhanced kinetic fractionation under continental air masses. A consistently negative $\delta^{18}\text{O}$ – $\Delta^{17}\text{O}$ relationship was observed except in winter when it weakened. This integrated analysis of $\delta^{18}\text{O}$, d-excess, and $\Delta^{17}\text{O}$ provides a comprehensive picture of source humidity, transport dynamics, and seasonal precipitation processed in a mid-latitude East Asia, and offers a valuable reference for refining isotope-enabled climate models over East Asia.

Global climate change has modified the hydrological cycle and increased the frequency of extreme weather events such as droughts and floods (Masson-Delmotte et al., 2021; Trenberth, 2011). In particular, Asia has experienced substantial changes in precipitation intensity and distribution over recent decades, coinciding with continuous surface temperature rise (Masson-Delmotte et al., 2021). Therefore, understanding precipitation processes, which form a critical link between the climate system and water resource management (Masson-Delmotte et al., 2021; Trenberth, 2011), is essential. In this context, stable isotopes ($\delta^{18}\text{O}$ and $\delta^2\text{H}$) in precipitation have emerged as powerful tracers of atmospheric water cycling and climate dynamics (Araguás-Araguás et al., 1998; Craig, 1961; Craig and Gordon, 1965; Dansgaard, 1964; Gat, 1996). In recent years, high-resolution isotope datasets have been increasingly recognized for understanding precipitation characteristics and isotopic responses in East Asia, as they are sensitive to isotopic fractionation during phase changes such as evaporation, condensation, and precipitation formation (Bowen et al., 2018; Cappa et al., 2003; Conroy et al., 2016; Craig and Gordon, 1965; Gat, 1996; Majoube, 1971).

The stable isotope composition of precipitation is strongly influenced by isotopic fractionation during phase changes such as evaporation, condensation, and precipitation formation. Heavier isotopes (^{18}O and ^2H) are preferentially removed or enriched depending on the atmospheric conditions, and the strength of this fractionation varies with environmental parameters such as temperature, relative humidity, and precipitation amount (Conroy et al., 2016; Craig and Gordon, 1965; Gat, 1996). Two well-known relationships, the temperature effect, where colder temperatures lead to lower $\delta^{18}\text{O}$ and $\delta^2\text{H}$ values, and the amount effect, where increased rainfall results in isotope depletion of stable water isotope, have been widely observed in various climate regimes (Araguás-Araguás et al., 1998; Dansgaard, 1964). These relationships have established $\delta^{18}\text{O}$ and $\delta^2\text{H}$ as powerful diagnostic tools for hydrological and climatological studies, as well as paleoclimate reconstructions (Jouzel et al., 1997; Winkler et al., 2012). However, the stable isotopic composition of precipitations ($\delta^{18}\text{O}$ and $\delta^2\text{H}$) are governed by both equilibrium and kinetic fractionations during phase changes such as evaporation and condensation, making them difficult to isolate the relative contributions of each process. In addition to $\delta^{18}\text{O}$ and $\delta^2\text{H}$, $\delta^{17}\text{O}$ can also be measured because $\delta^{17}\text{O}$ behaves almost proportionally to $\delta^{18}\text{O}$ under equilibrium conditions, simultaneous measurement of the two enables the quantification of subtle deviations arising from kinetic and non-equilibrium processes, forming the basis of triple oxygen isotope ($\delta^{17}\text{O}$, $\delta^{18}\text{O}$ and $\delta^2\text{H}$) studies (Angert et al., 2004; Luz and Barkan, 2010). Secondary parameters, namely deuterium excess (d-excess; $d - excess(\text{‰}) = \delta^2\text{H} - 8 \times \delta^{18}\text{O}$; defined by Dansgaard, 1964) and ^{17}O -excess ($\Delta^{17}\text{O}$; $\Delta^{17}\text{O} = \ln(\delta^{17}\text{O} + 1) - 0.528 \times \ln(\delta^{18}\text{O} + 1)$; defined by Luz and Barkan, 2010) are primarily sensitive to kinetic fractionation processes and thus help to disentangle them. While $\delta^{18}\text{O}$ and $\delta^2\text{H}$ mainly record equilibrium fractionation, d-excess and ^{17}O -excess reflect deviations from equilibrium associated with non-steady-state evaporation, vapor mixing, or supersaturation during cloud formation (Gat, 1996; Uemura et al., 2008). Meanwhile, $\Delta^{17}\text{O}$, defined as the logarithmic deviation from the global meteoric water line between $\delta^{17}\text{O}$ and $\delta^{18}\text{O}$, responds to non-equilibrium processes such as water vapor mixing and supersaturated condensation and

provides unique information about the dynamical history of atmospheric moisture (Barkan and Luz, 2007; Benetti et al., 2014; Landais et al., 2008). Recent analytical advances have enabled high-precision $\Delta^{17}\text{O}$ measurements, making this parameter a promising tracer of kinetic isotopic effects in the atmosphere. However, observational datasets for $\Delta^{17}\text{O}$ remain scarce in mid-latitude East Asia, and few studies have explored its co-variability with d-excess in this region. This study addresses these gaps by analyzing d-excess and $\Delta^{17}\text{O}$ in mid-latitude precipitation to better constrain the seasonal behavior and origin of precipitation over the Korean Peninsula.

Mid-latitude regions such as the Korean Peninsula exemplify the complex climatic controls on precipitation isotopes (Ha et al., 2012; Huang et al., 2007; Kim et al., 2019; J. Lee et al., 2013, K. Lee et al., 2003). The peninsula lies at the convergence between extratropical westerlies and the East Asian monsoon, resulting in large seasonal differences in moisture sources. In summer, moisture-rich air masses from subtropical oceans (e.g., the western North Pacific) dominate, bringing heavy monsoonal rainfall. This often yields an amount-effect signal where $\delta^{18}\text{O}$ values decrease during periods of high precipitation. In contrast, winter precipitation is dominated by cold, dry continental air from the Siberian-Mongolian High, which acquires limited moisture while crossing the Yellow Sea. As a result, winter precipitation is typically more $\delta^{18}\text{O}$ -depleted due to the lower temperatures and higher upstream rainout. These seasonal contrasts produce a strong annual cycle in precipitation isotope composition in the region, which is highly diagnostic of monsoon strength, moisture source changes, and temperature variability. Accordingly, long-term changes in precipitation isotopes (e.g., $\delta^{18}\text{O}$, $\delta^2\text{H}$, and $\Delta^{17}\text{O}$) may indicate broader hydrological and climatic changes. $\Delta^{17}\text{O}$ measurements offer additional diagnostic value as they are largely temperature-independent, reflecting kinetic fractionation sensitive to the relative humidity at the moisture source, for example, changes occurring during vapor formation or moisture recycling processes (Landais et al., 2008; Luz and Barkan, 2010). This makes $\Delta^{17}\text{O}$ a powerful complementary tracer for detecting subtle changes in atmospheric circulation and regional hydrological processes.

Despite their importance, long-term records of precipitation isotopes over the Korean Peninsula remain limited. The Global Network for Isotopes in Precipitation (GNIP), established in the 1960s, provides baseline data at a global scale; however, its coverage in East Asia is sparse and often discontinuous (Aggarwal et al., 2010). This lack of high-resolution, continuous isotope data limits the understanding of hydrological processes in the Korean Peninsula and their response to climate variability and change. To address this, in this study, a high-temporal-resolution, 5-year record of monthly triple oxygen and hydrogen isotopes in precipitation was obtained over the Korean Peninsula to investigate their seasonal and interannual variability in this mid-latitude setting. The results of this study provide a foundation for investigating moisture source dynamics, the behavior of isotope tracers such as d-excess and $\Delta^{17}\text{O}$, and the long-term isotopic response to climate variability in East Asia. These data are also essential for evaluating isotope-enabled climate models and interpreting regional paleoclimate proxies, and could accordingly enhance the understanding of hydroclimatic processes in monsoon-affected regions. By employing high-resolution,

ground-based isotope observations, this study provides a critical step toward refining the interpretation of atmospheric processes in mid-latitude monsoon-affected regions.

90 2 Study area and methods

The measurements were made approximately 30 km inland from the western coast of the Korean Peninsula, on the campus of Ewha Womans University in Seoul, South Korea (37°33'53" N, 126°56'46" E; Fig. 1A and B). The sampling point was located 80 m above sea level. The study area experiences a temperate monsoon climate, with large seasonal variations characterized by hot, humid summers driven by the East Asian summer monsoon (EASM) and cold, dry winters dominated by the Siberian High and the East Asian winter monsoon (Kim et al., 2019; Lee et al., 2013). The Korean Peninsula experiences a temperate monsoon climate with four distinct seasons, spring (March–May; MAM), summer (June–August; JJA), autumn (September–November; SON), and winter (December–February; DJF) (Ha et al., 2012; Lee et al., 2013). In summer, moist southwesterly winds bring heavy rainfall associated with the East Asian monsoon front, known regionally as the *Changma* in Korea peninsula, *Meiyu* in China, and *Baiu* in Japan, resulting in the concentration of annual precipitation within a few months. In winter, the strengthening of the extensive Siberian High pushes cold, dry air southward across the peninsula (Ding and Chan, 2005). Spring is generally mild and dry, whereas autumn is cooler and occasionally affected by typhoons or tropical storms that deliver intense rainfall events.

Precipitation samples were collected between January 2016 and December 2020 (five years) at approximately biweekly intervals. For each collection period, the deployment bottle remained in place to accumulate all precipitation events within the interval. No mineral oil was applied to prevent evaporation during precipitation collection, because the presence of organic compounds can interfere with spectroscopic isotope analysis in cavity ring-down systems. Previous studies have demonstrated that even trace amounts of organic contamination, such as mineral oil residues, can cause spectral interference and bias $\delta^2\text{H}$ and $\delta^{18}\text{O}$ measurements obtained by WS-CRDS (Gupta et al., 2009). Instead of using oil, we employed a funnel system that physically minimized post-collection evaporation. Precipitation was funneled directly into pre-cleaned and sealed PTFE bottles immediately after sampling period, thereby minimizing exposure to air and sunlight. Samples were collected on an unobstructed rooftop of a five-story building. This point was selected because its open setting, free from nearby buildings or vegetation, ensured that the collected precipitation was representative and minimally affected by local interference (Fig. 1C). All precipitation samples were stored in pre-cleaned HDPE bottles and sealed with Parafilm, and were kept frozen at $-20\text{ }^\circ\text{C}$ until preparation for analysis. Before isotope analysis, the samples were thawed, transferred to glass vials, and stored at $4\text{ }^\circ\text{C}$ in liquid form for less than two weeks prior to measurement.

All samples were transported in a frozen state to the Korea Polar Research Institute (KOPRI), where water isotope analysis was conducted using a wavelength-scanned cavity ring-down spectrometer (WS-CRDS; model L2140-I, Picarro Inc., CA, USA). The analytical protocol followed the optimized method of Kim et al. (2022) for high-precision triple oxygen isotope

measurements. For each vial, the instrument performed over 20 injections and only the five injections were averaged to
120 minimize memory effects. Samples and reference materials were prepared in duplicate vials; only the second vial was used for
evaluation, while the first served as a buffer against carryover effects. Of the total 20 injections per vial, only the final six were
used to calculate the average δ -values, in order to minimize memory effects from preceding samples. This strategy significantly
reduced the memory effects associated with isotopic differences between successive samples. Three international reference
waters (Vienna Standard Mean Ocean Water, Standard Light Antarctic Precipitation 2, Greenland Ice Sheet Precipitation) and
125 one in-house standard were used for Vienna Standard Mean Ocean Water (VSMOW)-SLAP scale normalization. At the
beginning of each analytical session, international reference waters (VSMOW2, SLAP2, and GISP) were measured for
VSMOW–SLAP scale normalization. Subsequently, samples were analyzed, and every ten samples, two in-house laboratory
standards (STYX and KT), both calibrated against VSMOW2 and SLAP2, were analyzed to monitor instrumental performance.
STYX, a natural water collected from the Styx Glacier region in Antarctica, was used to assess the long-term analytical
130 reproducibility of the WS-CRDS, while KT, a locally sourced tap water with isotopic composition similar to the precipitation
samples, was used to reduce potential memory effects during analysis. The long-term 1σ standard deviations obtained from
repeated STYX measurements over several years were $\pm 0.10\text{‰}$ for $\delta^2\text{H}$, $\pm 0.07\text{‰}$ for $\delta^{18}\text{O}$, and $\pm 0.01\text{‰}$ for $\delta^{17}\text{O}$, while the
1-year reproducibility for $\Delta^{17}\text{O}$ was ± 9 per meg (Kim et al., 2022). All data were reported relative to VSMOW using the delta
notation (δ) (Eq. (1)):

$$135 \quad \delta(\text{‰}) = \left(\frac{R_{\text{sample}}}{R_{\text{VSMOW}}} - 1 \right) \times 1000, \quad (1)$$

where R_{sample} and R_{VSMOW} represent the isotopic ratios of the sample (i.e., $^{18}\text{O}/^{16}\text{O}$, $^{17}\text{O}/^{16}\text{O}$, or $^2\text{H}/^1\text{H}$) and VSMOW, respectively.

To account for multiple precipitation events within a month, precipitation-weighted monthly means (δ_{wm}) were
calculated for $\delta^2\text{H}$, $\delta^{18}\text{O}$, and $\delta^{17}\text{O}$ as follows (Eq. (2)):

$$140 \quad \delta_{\text{wm}} = \frac{\sum P_i \times \delta_i}{\sum P_i} \quad (2)$$

where P_i is the precipitation amount and δ_i is the isotopic value for each event. Although precipitation samples were collected
at approximately 14-day intervals, all seasonal and intermonthly analyses in this study are based on precipitation-weighted
monthly mean values. For months with two biweekly samples, the isotope values were weighted by their corresponding
precipitation amounts to derive monthly means (δ_{wm}).

145 Meteorological data, including air temperature, relative humidity, and precipitation amount, were obtained from the
Korea Meteorological Administration (KMA) based on hourly observations at the Seoul station
(<https://www.weather.go.kr/w/index.do>). For each biweekly sampling interval, the hourly data corresponding to periods with

precipitation were integrated to derive time-weighted mean temperature and humidity and cumulative precipitation, representing the meteorological conditions relevant to each collected sample. The average monthly precipitation amount (grey bars) and average monthly temperature (black-lined boxes) for Seoul, based on these KMA data, are shown in Fig. 2.

3 Results and Discussion

3.1 Variations in precipitation stable isotopes

A total of 130 precipitation samples were collected during the study period. Precipitation-weighted monthly mean values were calculated from the biweekly samples and used for all subsequent analyses. The measured isotopic compositions of precipitation varied considerably: $\delta^{17}\text{O}$ ranged from -0.89 to -7.53‰ (average: -3.74‰); $\delta^{18}\text{O}$ from -1.74 to -14.25‰ (average: -7.11‰); and $\delta^2\text{H}$ from -11.8 to -93.5‰ (average: -45.2‰). The d-excess fluctuated between 23.7 and 2.1‰ (average: 11.7‰), whereas ^{17}O -excess ranged from 56 to -10‰ (average: 18‰). For all three parameters ($\delta^{17}\text{O}$, $\delta^{18}\text{O}$ and $\delta^2\text{H}$), the precipitation isotopic values were relatively depleted during the coldest months (December to February), increased between around March and April as condition warmed, and then sharply decreased between June and August, when precipitation peaked (Fig. 3). This pattern indicates a strong interplay between temperature effects and rainfall intensity in shaping the isotope signals. The monthly isotopic patterns observed during the study period align with those reported for Jeju Island in the Korean Peninsula and the Yangtze River region in China (Gou et al., 2022; Shin et al., 2021), suggesting that these regions may be influenced by similar meteorological patterns over East Asia. A distinct seasonal variation in d-excess is evident from the box plots (Fig. 3), with higher values in winter (particularly January and February; whole winter median values of $15\text{--}20\text{‰}$) and lower values in summer (medians: $0\text{--}5\text{‰}$). This pattern is consistent with previous findings in the Korean Peninsula and reflects the sensitivity of d-excess to relative humidity and non-equilibrium fractionation processes driven by moisture-source conditions (Kim et al., 2019; Lee and Kim, 2007). In winter, cold, dry air and a steep temperature/humidity gradient between the atmosphere and the ocean (or other moisture sources) enhance evaporation-driven fractionation, thereby elevating d-excess. Conversely, in summer, high relative humidity and abundant precipitation suppress these fractionation effects, resulting in substantially lower d-excess.

Unlike d-excess, which peaked in winter (median $\approx 17\text{‰}$) and reached its lowest values in summer (median $\approx 6\text{‰}$), ^{17}O -excess displayed a distinct seasonal pattern, being highest in spring (up to ≈ 40 per meg) and lowest in summer (down to ≈ 10 per meg). This contrast indicates that ^{17}O -excess and d-excess are influenced by different kinetic fractionation processes operating under distinct seasonal humidity regimes. It subsequently rose again in autumn, revealing a clear seasonal pattern of high ^{17}O -excess during the cold and/or dry seasons (spring, autumn, and winter) and lower values during the warm and humid summer period. The increase in ^{17}O -excess during winter and early spring suggests that vapor sourced from drier air masses (e.g., continental or high-latitude oceanic regions) undergoes more pronounced kinetic fractionation, primarily occurring during oceanic evaporation under low relative humidity, becomes more pronounced when vapor is sourced from drier air

masses such as continental or high-latitude oceanic regions. Overall, the sine fit of the average monthly ^{17}O -excess values ($R^2 = 0.53$) supports the above interpretation; although not perfectly periodic, it exhibits a distinct seasonal cycle, peaking in winter to early spring and reaching its minimum in summer.

3.2 Local Meteoric Water Line

The linear relationship between the precipitation $\delta^{18}\text{O}$ and $\delta^2\text{H}$ defines a Local Meteoric Water Line (LMWL) that closely aligns with the Global Meteoric Water Line (GMWL; Craig, 1961), while exhibiting additional seasonal variations (Fig. 4). The LMWL derived from linear regression is $\delta^2\text{H} = 7.87 (\pm 0.33) \cdot \delta^{18}\text{O} + 11.12 (\pm 2.57)$ ($R^2 = 0.93$), indicating that the isotopic composition of precipitation in Seoul follows the global meteoric trend that reflects equilibrium fractionation on average, although substantial seasonal variations in d-excess demonstrate the coexistence of kinetic effects that partially compensate in the annual regression. The near-identical slope to the GMWL suggests minimal deviation from global meteoric trends, although seasonal changes in moisture sources and humidity may introduce modest variation. Further examination of seasonal subsets revealed distinct differences in isotopic behavior across the year. Summer precipitation clusters tightly along the GMWL, indicating near-equilibrium condensation under humid monsoonal conditions. This pattern is consistent with the dominance of moisture originating from the Northwest Pacific and South China Sea, where high humidity minimizes kinetic fractionation effects. Conversely, winter precipitation plots above the GMWL, with a higher intercept (~ 22) compared to summer, reflecting the influence of cold, dry air masses and enhanced d-excess.

This difference between summer and winter precipitation suggests that kinetic fractionation, likely associated with ice-phase microphysics and dry air mass transport from the Asian continent, plays a greater role in winter precipitation compared to summer (Kim et al., 2019; Merlivat and Jouzel, 1979; Uemura et al., 2008). Spring and autumn values fall between these seasonal extremes, maintaining an overall LMWL slope close to 8. The persistence of a near-global slope across seasons indicates that equilibrium fractionation dominates the isotopic system; however, modest seasonal variations in intercept reflect differences in humidity and the moisture source over the year. These findings align with previous studies conducted in Korea based on year-long precipitation isotope records from Jeju, Hongseung and Busan, which reported LMWL slopes ranging from 7.3 to 8.4 and intercepts from 11.3 to 19.2 (Lee et al., 2003; Shin et al., 2021; Yoon and Koh, 2021). Compared to these, the LMWL in this study shows a similar slope but a slightly lower intercept. This confirms that, while Korean precipitation follows global meteoric trends, seasonal shifts in air mass origin and fractionation processes introduce predictable deviations from these trends (Lee et al., 2007; Lim et al., 2012; Shin et al., 2021; Yoon and Koh, 2021).

The correlation between $\delta^{17}\text{O}$ and $\delta^{18}\text{O}$ in natural waters has been well-established to follow a nearly linear relationship under equilibrium conditions (Angert et al., 2004; Landais et al., 2008; Luz and Barkan, 2011). This relationship is a fundamental characteristic of stable oxygen isotopes in precipitation, with minor deviations due to kinetic effects, ice-phase processes, and variations in relative humidity at the moisture source (Barkan and Luz, 2005). In the present study, the

210 relationship between precipitation $\delta^{17}\text{O}$ and $\delta^{18}\text{O}$ defines an LMWL, exhibiting strong linearity across all samples, although including seasonal variability (Supplementary Table 1). A linear regression applied to the full dataset results in $\delta^{17}\text{O} = 0.528 \cdot \delta^{18}\text{O} + 0.0105$ ($R^2 = 1.00$), confirming the strong linear correlation between $\delta^{17}\text{O}$ and $\delta^{18}\text{O}$ characteristic of mass-dependent fractionation in meteoric waters. A distinct separation in slope occurs when precipitation is classified into winter and non-winter periods: The higher $\delta^{17}\text{O}$ and $\delta^{18}\text{O}$ slopes in winter precipitation reflect enhanced kinetic fractionation under
215 cold and dry conditions, where low humidity amplifies non-equilibrium effects during condensation (Luz and Barkan, 2011). In this season, Rayleigh distillation along moisture transport pathways further depletes heavy isotopes in precipitation, increasing the $\delta^{17}\text{O}$ and $\delta^{18}\text{O}$ slope, a pattern also observed in high-latitude precipitation (Landais et al., 2012). Ice-phase microphysical processes, particularly supersaturation with respect to ice, cause additional fractionation, reinforcing the seasonal difference in the slope of $\delta^{17}\text{O}$ vs $\delta^{18}\text{O}$ regression line (Luz and Barkan, 2010). In contrast, non-winter precipitation
220 follows near-equilibrium fractionation, with high humidity minimizing kinetic effects and maintaining $\delta^{17}\text{O}$ – $\delta^{18}\text{O}$ ratios similar to those of global meteoric waters (Angert et al., 2004; Landais et al., 2008). These seasonal variations highlight the role of atmospheric humidity and cloud microphysics in modulating triple oxygen isotope fractionation.

The $\delta^{17}\text{O}$ – $\delta^{18}\text{O}$ regression derived from the Seoul dataset ($\delta^{17}\text{O} = 0.528 \times \delta^{18}\text{O} + 0.0205$; $R^2 = 1.00$) is consistent with results from a nearby GNIP station at Cheongju (~100 km south), which reported $\delta^{17}\text{O} = 0.5283 \times \delta^{18}\text{O} + 0.0216$ (Terzer-
225 Wassmuth et al., 2023). Both stations exhibit nearly identical slopes, but the Cheongju record shows a slightly higher intercept (~11 per meg difference), likely reflecting its more continental location and lower ambient humidity under the influence of the Siberian High, whereas Seoul's stronger maritime influence and higher boundary-layer humidity suppress kinetic fractionation (Landais et al., 2010; Li et al., 2015; Uemura et al., 2008). This small offset lies within the regional variability observed across East Asia and supports the interpretation that both datasets represent the same large-scale atmospheric processes. Taken
230 together, the Seoul record displays an LMWL slope consistent with global meteoric trends while its intercepts and the triple-oxygen isotope relationship align closely with nearby GNIP observations. This coherence demonstrates that the isotopic variability observed in Seoul is regionally representative and primarily governed by seasonal changes in humidity, moisture-source origin, and kinetic fractionation strength.

3.3 Climatic controls on precipitation isotope composition

235 This study performed a seasonal correlation analysis between precipitation isotopes ($\delta^2\text{H}$, $\delta^{18}\text{O}$, d-excess, and ^{17}O -excess) and meteorological parameters (air temperature, relative humidity, precipitation amount) (Fig. 5). The overall monthly averages across the study period revealed a significant correlation between meteorological variables and isotopes only for d-excess. This suggests that variations in $\delta^{18}\text{O}$ and ^{17}O -excess are governed by different meteorological influences that vary with season. In contrast, d-excess consistently exhibited significant negative correlations with relative humidity, temperature, and
240 precipitation. These relationships can be attributed to a combination of factors: lower relative humidity and temperature at the moisture source enhance kinetic fractionation during evaporation, thereby increasing d-excess (Merlivat and Jouzel, 1979;

Uemura et al., 2008), while locally, higher temperatures and lower humidity may promote re-evaporation and mixing of moist and dry air masses, which reduce d-excess (Steen-Larsen et al., 2014). The negative correlation with precipitation may reflect the amount effect, but is better interpreted as a result of multiple interacting meteorological factors—such as variations in temperature, relative humidity, air-mass trajectories, precipitation intensity, and microphysical processes within clouds—that together influence the isotopic composition of precipitation (Holmes et al., 2024).

In spring, strong positive correlations were observed between $\delta^{18}\text{O}$ values and both temperature and precipitation ($r = 0.49$ and 0.53 , respectively; $n = 10$ in each case). This indicates a significant temperature effect during spring due to relatively dry conditions and intermittent precipitation. The d-excess also displayed strong negative correlations with temperature during this period, providing insights into moisture sources and isotopic fractionation during precipitation (Uemura et al., 2008). During summer, $\delta^{18}\text{O}$ values was significantly negatively correlated with precipitation amount ($r = -0.44$, $n = 14$), reflecting the amount-effect that is typical in monsoon climates. Increased relative humidity during summer resulted in more frequent rainfall events, contributing to lower $\delta^{18}\text{O}$ values. Furthermore, the relatively low $\delta^{18}\text{O}$ values observed in summer, compared with other months of the year, primarily reflect the amount effect associated with prolonged monsoon precipitation and successive rainout within moisture-rich air masses of marine origin. In autumn, the monthly mean $\delta^{18}\text{O}$ was strongly negatively correlated with precipitation amount ($r = -0.55$, $n = 10$), mainly due to frequent heavy rainfall events associated with typhoons or tropical cyclones, which are most common during this season. Although there were no direct passages of typhoons at the study site during the study period, substantial precipitation events influenced by typhoons were frequently observed. The strong correlations observed between d-excess and meteorological variables likely reflect moisture supply from nearby oceanic areas influenced by migratory high-pressure systems. In winter, d-excess and $\Delta^{17}\text{O}$ exhibited a clear negative correlation with meteorological variables such as temperature and precipitation amount, strongly reflecting evaporation conditions and the characteristics of moisture sources from the nearby ocean.

The results of this study indicate that seasonal variations in precipitation isotopes in Korea are closely linked to local meteorological factors such as temperature, relative humidity, and precipitation amount (Dansgaard, 1964; Lee et al., 2013) and reflect distinct seasonal regimes shaped by synoptic-scale circulation patterns (Ha et al., 2012; Huang et al., 2007). The findings indicate that, in summer, isotopic depletion is primarily governed by the amount effect under the influence of the East Asian monsoon, which delivers warm, moisture-rich air masses and produces intense rainfall events (Lee et al., 2003; Yu et al., 2006). Spring exhibits more variable isotopic signals due to transitional moisture sources and fluctuating atmospheric conditions, which result in a combination of continental and maritime influences. In autumn, isotopic variability is often enhanced by episodic typhoons, which introduce large volumes of isotopically light precipitation associated with strong convective activity. In contrast, winter precipitation is strongly depleted in heavy isotopes and enriched in d-excess due to the presence of cold, dry continental air masses advected by the East Asian winter monsoon (Kim et al., 2019; Lee et al., 2003).

This seasonal variation underscores the role of changing moisture origins and precipitation mechanisms in modulating the stable isotope composition of precipitation across the Korean Peninsula.

275 3.4 Interpreting seasonal decoupling of $\Delta^{17}\text{O}$ and d-excess

Variations in the $\Delta^{17}\text{O}$ and d-excess of meteoric water are primarily governed by kinetic fractionation, making them reliable indicators of relative humidity at the moisture source (Barkan and Luz, 2007; Landais et al., 2010; Pfahl and Sodemann, 2014; Uemura et al., 2008). However, when measured in precipitation, these isotope indices may also reflect complex post-
280 evaporation processes such as continental recycling, partial re-evaporation within clouds, and sub-cloud raindrop evaporation (Landais et al., 2010; Li et al., 2015; Tian et al., 2018; Xia et al., 2023). These additional factors complicate the interpretation of seasonal isotopic variability in precipitation (Aron et al., 2023; Chen et al., 2023).

Our analysis showed that, during spring, summer, and autumn, $\Delta^{17}\text{O}$ was moderately negatively correlation with $\delta^{18}\text{O}$ and weakly positively correlated with d-excess (Fig. 6). These tendencies are broadly consistent with theoretical expectations under non-steady-state evaporation, where kinetic fractionation induces a simultaneous increase in $\Delta^{17}\text{O}$ and d-excess and a
285 depletion in $\delta^{18}\text{O}$ (Li et al., 2015). The slopes observed between $\Delta^{17}\text{O}$ and d-excess fall within the range of 0.7–2.0 per meg per ‰, which aligns with results from conceptual models and field-based estimates in regions influenced by oceanic moisture (Landais et al., 2010; Li et al., 2015). These observations suggest that, in non-winter seasons, kinetic processes such as evaporation and sub-cloud re-evaporation exert a dominant influence on isotopic composition. In contrast, in winter precipitation, no statistically significant correlation was observed between $\Delta^{17}\text{O}$ and either $\delta^{18}\text{O}$ or d-excess. While the d-
290 excess range remained relatively narrow in winter, $\Delta^{17}\text{O}$ values showed a larger dispersion in this season (Fig. 3). This variability likely reflects multiple processes operating simultaneously under cold, dry atmospheric conditions. First, $\Delta^{17}\text{O}$ is inherently more sensitive to vapor mixing and nonequilibrium effects than d-excess, and may therefore decouple from $\delta^{18}\text{O}$ -based processes under reduced surface moisture recycling (Li et al., 2015; Xia et al., 2023) Second, part of the enhanced winter $\Delta^{17}\text{O}$ variability may also arise from ice–vapor equilibrium fractionation during snow formation, which affects $\Delta^{17}\text{O}$ and d-
295 excess differently from liquid-phase condensation (Jouzel and Merlivat, 1984; Landais et al., 2012). Under such mixed-phase conditions, equilibrium enrichment associated with ice deposition can increase $\Delta^{17}\text{O}$ while kinetic effects during vapor transport or re-evaporation act in the opposite direction, producing the wide isotopic dispersion observed in winter samples. Taken together, these results indicate that winter isotopic variability in precipitation is governed not only by mid-tropospheric vapor mixing and heterogeneous moisture sources but also by ice-phase fractionation processes that accompany snow
300 formation, which are difficult to isolate in biweekly integrated samples.

The results further indicate that $\Delta^{17}\text{O}$ is negative correlated with $\delta^{18}\text{O}$ but positively correlated with d-excess during spring, summer, and autumn, consistent with theoretical expectations under non-steady-state evaporation conditions. These correlations reflect the influence of kinetic fractionation processes such as evaporation and sub-cloud re-evaporation, with

$\Delta^{17}\text{O}$ -d-excess slopes (0.7–2.0 per meg per ‰) aligning with previous modeling and observational studies (Landais et al., 2010; Li et al., 2015). In contrast, winter precipitation showed no significant correlations between $\Delta^{17}\text{O}$, $\delta^{18}\text{O}$, and d-excess, and moreover, showed increased $\Delta^{17}\text{O}$ variability compared to the other seasons, suggesting a greater sensitivity to vapor mixing and reduced surface recycling. Overall, these findings demonstrate the utility of $\Delta^{17}\text{O}$, alongside $\delta^{18}\text{O}$ and d-excess, in disentangling the effects of evaporation, recycling, and mixing on precipitation isotopes across seasons.

3.5 Seasonal Comparison of Precipitation Isotope Trends: Observations vs. Iso-GSM Model

Figure 7 compares the monthly mean stable isotope values ($\delta^2\text{H}$ and $\delta^{18}\text{O}$) and d-excess in precipitation from this study (black line/gray shading) with those simulated by Isotope-enabled Global Spectral Model (Iso-GSM; red line/pink shading). Both datasets reproduce the same broad seasonal patterns, with isotopically depleted summer precipitation and enriched winter values. However, some systematic differences are apparent. The Iso-GSM outputs are slightly more depleted in $\delta^2\text{H}$ and $\delta^{18}\text{O}$, especially during late autumn and winter and exhibit a narrower range of d-excess variability compared to the observations. These discrepancies likely reflect known limitations of isotope-enabled GCMs in representing kinetic fractionation processes and moisture recycling dynamics, particularly during cold-season conditions (Pfahl and Sodemann, 2014; Risi et al., 2008). While the Iso-GSM captures the overall phasing of the seasonal isotope cycle, it tends to underestimate the amplitude of d-excess fluctuations, which are strongly influenced by sub-cloud evaporation, boundary-layer humidity, and re-evaporation of falling raindrops. The observed dataset, by contrast, shows pronounced intra-annual variability in d-excess (ranging from approximately 5 to 20‰), especially outside the winter season, highlighting processes that are only partially represented in the model framework.

It is important to note that this comparison is intended as an illustrative example of how the Seoul isotope dataset can be used to benchmark model outputs rather than as a full-scale model evaluation. The observed model–data differences underscore how high-temporal-resolution isotope measurements can help identify the physical processes that require better parameterization in isotope-enabled models, such as cloud–precipitation interactions, moisture-source tracking, and convective transport. Moreover, expanding future model, data comparisons to include triple oxygen isotope measurements ($\Delta^{17}\text{O}$) could provide an additional constraint for evaluating non-equilibrium and mixing effects that are difficult to isolate using $\delta^{18}\text{O}$ and d-excess alone (Luz and Barkan, 2010; Landais et al., 2008). This highlights the potential of the present dataset as a regional benchmark for improving isotope-enabled model parameterizations and for guiding future collaborations aimed at incorporating $\Delta^{17}\text{O}$ into global model simulations.

5 Conclusions

This study examined 130 precipitation samples collected in Seoul between 2016 and 2020 to quantify seasonal variability in $\delta^2\text{H}$, $\delta^{18}\text{O}$, $\delta^{17}\text{O}$, d-excess, and $\Delta^{17}\text{O}$ and clarify how these isotope tracers respond to local meteorological conditions. $\delta^{17}\text{O}$,

335 $\delta^{18}\text{O}$, and $\delta^2\text{H}$ followed a pronounced sinusoidal seasonal cycle, being most depleted during winter, becoming gradually
enriched in spring, and sharply declining during the summer monsoon due to the amount effect. d-excess was highest in winter
and lowest in summer, reflecting its sensitivity to non-equilibrium evaporation and relative humidity at the moisture source.
Meanwhile, $\Delta^{17}\text{O}$ showed a similar seasonal cycle, although with reduced amplitude, highlighting its additional sensitivity to
340 large-scale circulation and vapor transport. The calculated Local Meteoric Water Line ($\delta^2\text{H} = 7.87 \cdot \delta^{18}\text{O} + 11.1$) closely
resembles the Global Meteoric Water Line, but with a higher winter intercept, suggesting enhanced ice-phase fractionation
and the influence of dry continental air masses. The $\delta^{17}\text{O}$ – $\delta^{18}\text{O}$ relationship confirmed mass-dependent fractionation across the
dataset; however, the slope steepened during winter, indicating stronger kinetic effects under low humidity.

The comparison of the seasonal behavior of $\delta^{18}\text{O}$, d-excess, and $\Delta^{17}\text{O}$ revealed distinct tracer-specific responses. During
spring, summer, and autumn, $\Delta^{17}\text{O}$ was negatively correlated with $\delta^{18}\text{O}$ and positively correlated with d-excess, consistent
with theoretical expectations for non-steady-state evaporation. The slope between $\Delta^{17}\text{O}$ and d-excess ranged from 0.7 to 2.0
345 per meg per ‰, aligning with conceptual models and empirical results from ocean-influenced regions. In contrast, in winter,
no statistically significant correlation was observed between $\Delta^{17}\text{O}$ and either $\delta^{17}\text{O}$ or d-excess, while $\Delta^{17}\text{O}$ displayed greater
dispersion to compared to the other season. This decoupling likely reflects the heightened sensitivity of $\Delta^{17}\text{O}$ to mid-
tropospheric vapor mixing and contributions from diverse moisture sources, rather than surface evaporation alone. These
findings underscore the utility of $\Delta^{17}\text{O}$ as a diagnostic tracer of atmospheric mixing and moisture transport, especially in cold
350 seasons.

By integrating $\delta^{18}\text{O}$, d-excess, and $\Delta^{17}\text{O}$, this study provides a more comprehensive understanding of seasonal
hydrological processes than would be possible using any of these tracers alone. The results highlight key controls on isotopic
variability in the East Asian monsoon system, particularly during winter, when interactions between continental and marine
air masses become dominant. This dataset serves as a valuable benchmark for interpreting modern hydroclimatic dynamics
355 and offers a foundation for evaluating isotope-enabled climate models. Beyond contemporary climate diagnostics, the
integrated use of $\Delta^{17}\text{O}$ and d-excess also holds implications for interpreting isotope records in subsurface hydrological archives.
These tracers may enable enhanced reconstructions of past climatic conditions from speleothems or glacier ice and improve
the understanding of groundwater recharge processes in monsoon-influenced regions. As such, this work bridges modern
atmospheric processes with paleoclimate interpretations and supports future hydroclimate modeling and water resource
360 management across East Asia.

Financial support. This research was supported by the Korea Polar Research Institute grant (PE25100) and the National
Research Foundation of Korea grant funded by the Korean Government (NRF2022R1A2C3007047). Additional support was
provided by the Korea Environment Industry & Technology Institute (KEITI) through Aquatic Ecosystem Conservation
Research Program, funded by the Korea Ministry of Environment (MOE) (RS-2024-00332851).

365 References

- Aggarwal, P. K., Araguás-Araguás, L. J., Groening, M., Kulkarni, K. M., Kurttas, T., Newman, B. D., and Vitvar, T.: Global Hydrological Isotope Data and Data Networks, in: *Isoscapes: Understanding movement, pattern, and process on Earth through isotope mapping*, edited by: West, J. B., Bowen, G. J., Dawson, T. E., and Tu, K. P., Springer Netherlands, Dordrecht, 33–50, https://doi.org/10.1007/978-90-481-3354-3_2, 2010.
- 370 Angert, A., Cappa, C. D., and DePaolo, D. J.: Kinetic ^{17}O effects in the hydrologic cycle: Indirect evidence and implications, *Geochimica et Cosmochimica Acta*, 68, 3487–3495, <https://doi.org/10.1016/j.gca.2004.02.010>, 2004.
- Araguás-Araguás, L., Froehlich, K., and Rozanski, K.: Stable isotope composition of precipitation over southeast Asia, *J. Geophys. Res.*, 103, 28721–28742, <https://doi.org/10.1029/98JD02582>, 1998.
- Aron, P. G., Li, S., Brooks, J. R., Welker, J. M., and Levin, N. E.: Seasonal Variations in Triple Oxygen Isotope Ratios of
375 Precipitation in the Western and Central United States, *Paleoceanography and Paleoclimatology*, 38, e2022PA004458, <https://doi.org/10.1029/2022PA004458>, 2023.
- Barkan, E. and Luz, B.: High precision measurements of $^{17}\text{O}/^{16}\text{O}$ and $^{18}\text{O}/^{16}\text{O}$ ratios in H_2O , *Rapid Comm Mass Spectrometry*, 19, 3737–3742, <https://doi.org/10.1002/rcm.2250>, 2005.
- Barkan, E. and Luz, B.: Diffusivity fractionations of HO/HO and HO/HO in air and their implications for isotope hydrology,
380 *Rapid Comm Mass Spectrometry*, 21, 2999–3005, <https://doi.org/10.1002/rcm.3180>, 2007.
- Benetti, M., Reverdin, G., Pierre, C., Merlivat, L., Risi, C., Steen-Larsen, H. C., and Vimeux, F.: Deuterium excess in marine water vapor: Dependency on relative humidity and surface wind speed during evaporation, *JGR Atmospheres*, 119, 584–593, <https://doi.org/10.1002/2013JD020535>, 2014.
- Bowen, G. J., Putman, A., Brooks, J. R., Bowling, D. R., Oerter, E. J., and Good, S. P.: Inferring the source of evaporated
385 waters using stable H and O isotopes, *Oecologia*, 187, 1025–1039, <https://doi.org/10.1007/s00442-018-4192-5>, 2018.
- Cappa, C. D., Hendricks, M. B., DePaolo, D. J., and Cohen, R. C.: Isotopic fractionation of water during evaporation, *J. Geophys. Res.*, 108, 2003JD003597, <https://doi.org/10.1029/2003JD003597>, 2003.
- Chen, J., Chen, J., Zhang, X. J., Peng, P., and Risi, C.: A century and a half precipitation oxygen isoscape for China generated using data fusion and bias correction, *Sci Data*, 10, 185, <https://doi.org/10.1038/s41597-023-02095-1>, 2023.
- 390 Conroy, J. L., Noone, D., Cobb, K. M., Moerman, J. W., and Konecky, B. L.: Paired stable isotopologues in precipitation and vapor: A case study of the amount effect within western tropical Pacific storms, *JGR Atmospheres*, 121, 3290–3303, <https://doi.org/10.1002/2015JD023844>, 2016.
- Craig, H.: Isotopic Variations in Meteoric Waters, *Science*, 133, 1702–1703, <https://doi.org/10.1126/science.133.3465.1702>, 1961.
- 395 Craig, H. and Gordon, L. I.: Deuterium and oxygen 18 variations in the ocean and the marine atmosphere, in: *Stable Isotopes in Oceanographic Studies and Paleotemperatures*, Pisa, Spoleto, Italy, 9–130, 1965.

- Dansgaard, W.: Stable isotopes in precipitation, *Tellus*, 16, 436–468, <https://doi.org/10.1111/j.2153-3490.1964.tb00181.x>, 1964.
- Gat, J. R.: OXYGEN AND HYDROGEN ISOTOPES IN THE HYDROLOGIC CYCLE, 1996.
- 400 Gupta, P., Noone, D., Galewsky, J., Sweeney, C., and Vaughn, B. H.: Demonstration of high-precision continuous measurements of water vapor isotopologues in laboratory and remote field deployments using wavelength-scanned cavity ring-down spectroscopy (WS-CRDS) technology, *Rapid Comm Mass Spectrometry*, 23, 2534–2542, <https://doi.org/10.1002/rcm.4100>, 2009.
- 405 Ha, K.-J., Heo, K.-Y., Lee, S.-S., Yun, K.-S., and Jhun, J.-G.: Variability in the East Asian Monsoon: a review, *Meteorological Applications*, 19, 200–215, <https://doi.org/10.1002/met.1320>, 2012.
- Holmes, J., Jourdan, Anne-Lise, and Darling, W. G.: Stable-isotope variability in daily precipitation: insights from a low-cost collector in SE England, *Isotopes in Environmental and Health Studies*, 60, 596–614, <https://doi.org/10.1080/10256016.2024.2402730>, 2024.
- Huang, R., Chen, J., and Huang, G.: Characteristics and variations of the East Asian monsoon system and its impacts on climate disasters in China, *Adv. Atmos. Sci.*, 24, 993–1023, <https://doi.org/10.1007/s00376-007-0993-x>, 2007.
- 410 Jouzel, J., Alley, R. B., Cuffey, K. M., Dansgaard, W., Grootes, P., Hoffmann, G., Johnsen, S. J., Koster, R. D., Peel, D., Shuman, C. A., Stievenard, M., Stuiver, M., and White, J.: Validity of the temperature reconstruction from water isotopes in ice cores, *J. Geophys. Res.*, 102, 26471–26487, <https://doi.org/10.1029/97JC01283>, 1997.
- 415 Kim, S., Han, Y., Hur, S. D., Yoshimura, K., and Lee, J.: Relating Moisture Transport to Stable Water Vapor Isotopic Variations of Ambient Wintertime along the Western Coast of Korea, *Atmosphere*, 10, 806, <https://doi.org/10.3390/atmos10120806>, 2019.
- Kim, S., Han, C., Moon, J., Han, Y., Hur, S. D., and Lee, J.: An optimal strategy for determining triple oxygen isotope ratios in natural water using a commercial cavity ring-down spectrometer, *Geosci J*, 26, 637–647, <https://doi.org/10.1007/s12303-022-0009-y>, 2022.
- 420 Landais, A., Barkan, E., and Luz, B.: Record of $\delta^{18}\text{O}$ and 17O -excess in ice from Vostok Antarctica during the last 150,000 years, *Geophysical Research Letters*, 35, 2007GL032096, <https://doi.org/10.1029/2007GL032096>, 2008.
- Landais, A., Risi, C., Bony, S., Vimeux, F., Descroix, L., Falourd, S., and Bouygues, A.: Combined measurements of 17O excess and d-excess in African monsoon precipitation: Implications for evaluating convective parameterizations, *Earth and Planetary Science Letters*, 298, 104–112, <https://doi.org/10.1016/j.epsl.2010.07.033>, 2010.
- 425 Landais, A., Ekaykin, A., Barkan, E., Winkler, R., and Luz, B.: Seasonal variations of 17O -excess and d-excess in snow precipitation at Vostok station, East Antarctica, *J. Glaciol.*, 58, 725–733, <https://doi.org/10.3189/2012JoG11J237>, 2012.
- Lee, J., Worden, J., Koh, D.-C., Yoshimura, K., and Lee, J.-E.: A seasonality of δD of water vapor (850–500 hPa) observed from space over Jeju Island, Korea, *Geosci J*, 17, 87–95, <https://doi.org/10.1007/s12303-013-0003-5>, 2013.
- 430 Lee, K., Grundstein, A., Wenner, D., Choi, M., Woo, N., and Lee, D.: Climatic controls on the stable isotopic composition of precipitation in Northeast Asia, *Clim. Res.*, 23, 137–148, <https://doi.org/10.3354/cr023137>, 2003.

- Lee, K.-S. and Kim, Y.: Determining the seasonality of groundwater recharge using water isotopes: a case study from the upper North Han River basin, Korea, *Environ Geol*, 52, 853–859, <https://doi.org/10.1007/s00254-006-0527-3>, 2007.
- Lee, K.-S., Kim, J.-M., Lee, D.-R., Kim, Y., and Lee, D.: Analysis of water movement through an unsaturated soil zone in Jeju Island, Korea using stable oxygen and hydrogen isotopes, *Journal of Hydrology*, 345, 199–211, <https://doi.org/10.1016/j.jhydrol.2007.08.006>, 2007.
- Li, S., Levin, N. E., and Chesson, L. A.: Continental scale variation in ^{17}O -excess of meteoric waters in the United States, *Geochimica et Cosmochimica Acta*, 164, 110–126, <https://doi.org/10.1016/j.gca.2015.04.047>, 2015.
- Lim, C., Lee, I., Lee, S.-M., Yu, J.-Y., and Kaufman, A. J.: Sulfur, oxygen, and hydrogen isotope compositions of precipitation in Seoul, South Korea, *Geochem. J.*, 46, 443–457, <https://doi.org/10.2343/geochemj.1.0173>, 2012.
- 435 Luz, B. and Barkan, E.: Variations of $^{17}\text{O}/^{16}\text{O}$ and $^{18}\text{O}/^{16}\text{O}$ in meteoric waters, *Geochimica et Cosmochimica Acta*, 74, 6276–6286, <https://doi.org/10.1016/j.gca.2010.08.016>, 2010.
- Luz, B. and Barkan, E.: The isotopic composition of atmospheric oxygen: ISOTOPIC COMPOSITION OF AIR OXYGEN, *Global Biogeochem. Cycles*, 25, n/a-n/a, <https://doi.org/10.1029/2010GB003883>, 2011.
- Majoube, M.: Fractionnement en oxygène 18 et en deutérium entre l'eau et sa vapeur, *Journal de Chimie Physique*, 68, 1423–
445 1436, <https://doi.org/10.1051/jcp/1971681423>, 1971.
- Masson-Delmotte, V., Panmao, Z., Anna, P., Sarah, L. C., Clotilde, P., Yang, C., Leah, G., Melissa, I. G., J.B. Robin, M., Sophie, B., Mengtian, H., Ozge, Y., Rong, Y., Baiquan, Z., Elisabeth, L., Thomas, K. M., Tim, W., Katherine, L., and Nada: Climate Change 2021 – The Physical Science Basis: Working Group I Contribution to the Sixth Assessment Report of the Intergovernmental Panel on Climate Change, 1st ed., Cambridge University Press, <https://doi.org/10.1017/9781009157896>,
450 2021.
- Merlivat, L. and Jouzel, J.: Global climatic interpretation of the deuterium-oxygen 18 relationship for precipitation, *J. Geophys. Res.*, 84, 5029–5033, <https://doi.org/10.1029/JC084iC08p05029>, 1979.
- Pfahl, S. and Sodemann, H.: What controls deuterium excess in global precipitation?, *Clim. Past*, 10, 771–781, <https://doi.org/10.5194/cp-10-771-2014>, 2014.
- 455 Risi, C., Bony, S., and Vimeux, F.: Influence of convective processes on the isotopic composition ($\delta^{18}\text{O}$ and δD) of precipitation and water vapor in the tropics: 2. Physical interpretation of the amount effect, *J. Geophys. Res.*, 113, 2008JD009943, <https://doi.org/10.1029/2008JD009943>, 2008.
- Shin, Y., Kim, T., Moon, S., Yun, S.-T., Moon, D., Han, H., and Kang, K.: A Study on the Recharge Characteristics of Groundwater in the Jeju Samdasoo Watershed Using Stable Water Isotope Data, *Journal of Soil and Groundwater Environment*,
460 26, 25–36, <https://doi.org/10.7857/JSGE.2021.26.3.025>, 2021.
- Steen-Larsen, H. C., Sveinbjörnsdóttir, A. E., Peters, A. J., Masson-Delmotte, V., Guishard, M. P., Hsiao, G., Jouzel, J., Noone, D., Warren, J. K., and White, J. W. C.: Climatic controls on water vapor deuterium excess in the marine boundary layer of the North Atlantic based on 500 days of in situ, continuous measurements, *Atmos. Chem. Phys.*, 14, 7741–7756, <https://doi.org/10.5194/acp-14-7741-2014>, 2014.

- 465 Tian, C., Wang, L., Kaseke, K. F., and Bird, B. W.: Stable isotope compositions ($\delta^2\text{H}$, $\delta^{18}\text{O}$ and $\delta^{17}\text{O}$) of rainfall and snowfall in the central United States, *Sci Rep*, 8, 6712, <https://doi.org/10.1038/s41598-018-25102-7>, 2018.
- Trenberth, K.: Changes in precipitation with climate change, *Clim. Res.*, 47, 123–138, <https://doi.org/10.3354/cr00953>, 2011.
- Uemura, R., Matsui, Y., Yoshimura, K., Motoyama, H., and Yoshida, N.: Evidence of deuterium excess in water vapor as an indicator of ocean surface conditions, *J. Geophys. Res.*, 113, 2008JD010209, <https://doi.org/10.1029/2008JD010209>, 2008.
- 470 Winkler, R., Landais, A., Sodemann, H., Dümbgen, L., Prié, F., Masson-Delmotte, V., Stenni, B., and Jouzel, J.: Deglaciation records of $\delta^{17}\text{O}$ -excess in East Antarctica: reliable reconstruction of oceanic normalized relative humidity from coastal sites, *Clim. Past*, 8, 1–16, <https://doi.org/10.5194/cp-8-1-2012>, 2012.
- Xia, Z., Surma, J., and Winnick, M. J.: The response and sensitivity of deuterium and ^{17}O excess parameters in precipitation to hydroclimate processes, *Earth-Science Reviews*, 242, 104432, <https://doi.org/10.1016/j.earscirev.2023.104432>, 2023.
- 475 Yoon, Y. Y. and Koh, D. C.: Tritium and stable isotope content variation in precipitation at Hongseung: West Korea Region, *J Radioanal Nucl Chem*, 330, 413–417, <https://doi.org/10.1007/s10967-021-07955-x>, 2021.
- Yu, W., Yao, T., Tian, L., Li, Z., Sun, W., and Wang, Y.: Relationships between $\delta^{18}\text{O}$ in summer precipitation and temperature and moisture trajectories at Muztagata, western China, *SCI CHINA SER D*, 49, 27–35, <https://doi.org/10.1007/s11430-004-5097-1>, 2006.

480

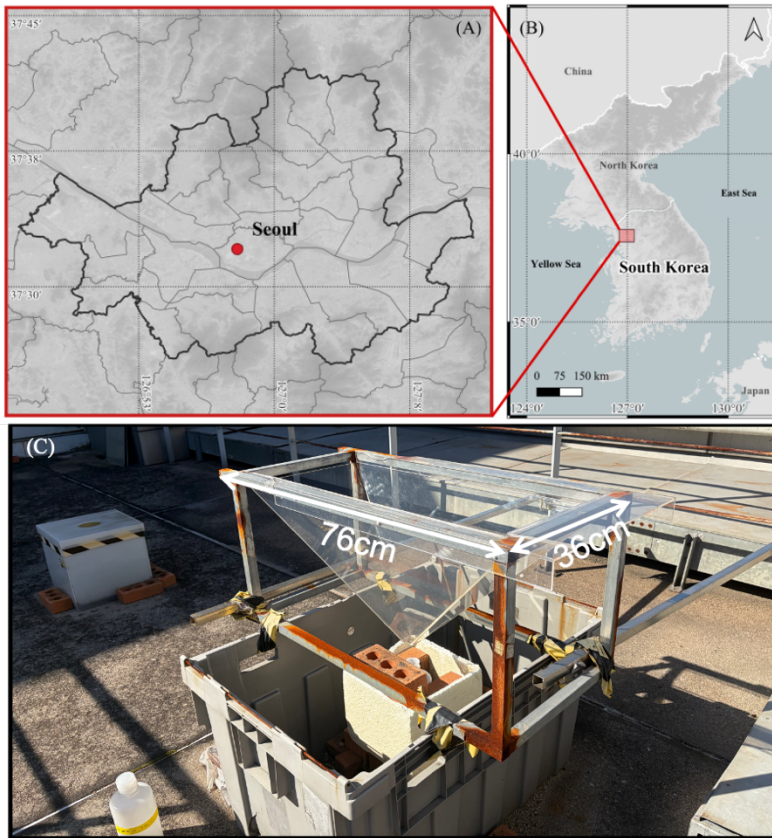


Figure 1: (A) A map showing the location of South Korea within East Asia. (B) An enlarged map highlighting the study site (red dot) in Seoul, South Korea, with administrative boundaries for surrounding regions. (C) The precipitation sampling device that was installed at the study site, designed to minimize post-collection evaporation.

485

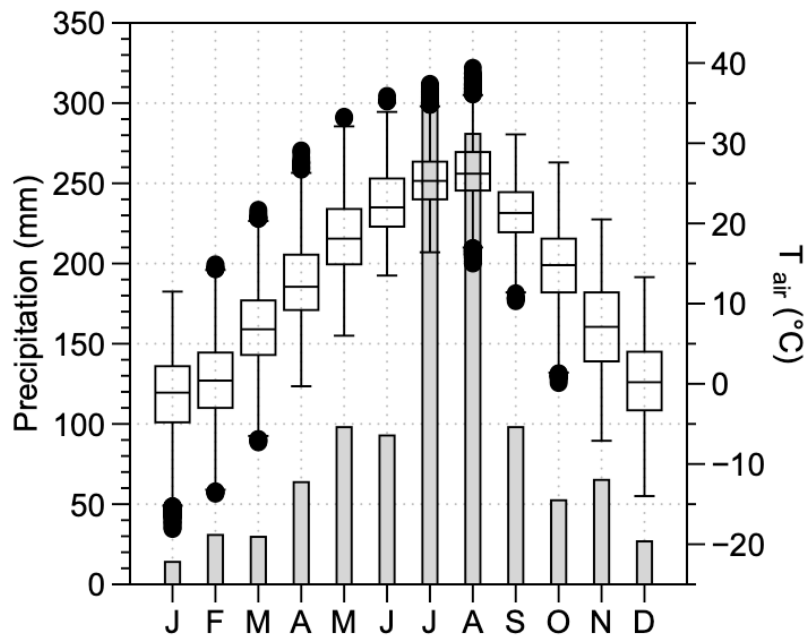


Figure 2: The average monthly precipitation amount (grey bars) and average monthly temperature (black-lined boxes) for the city of Seoul, based on meteorological data provided by the Korea Meteorological Administration (available at: <https://www.weather.go.kr/w/index.do>).

490

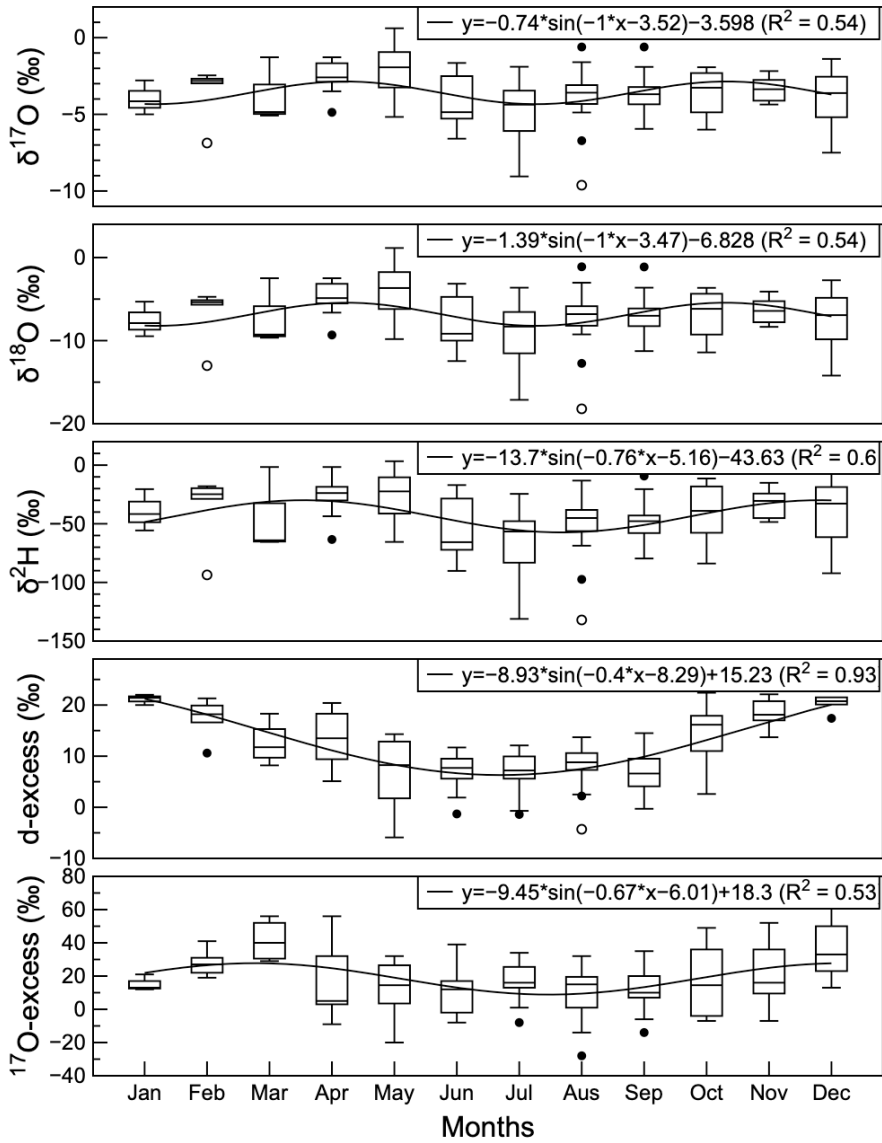
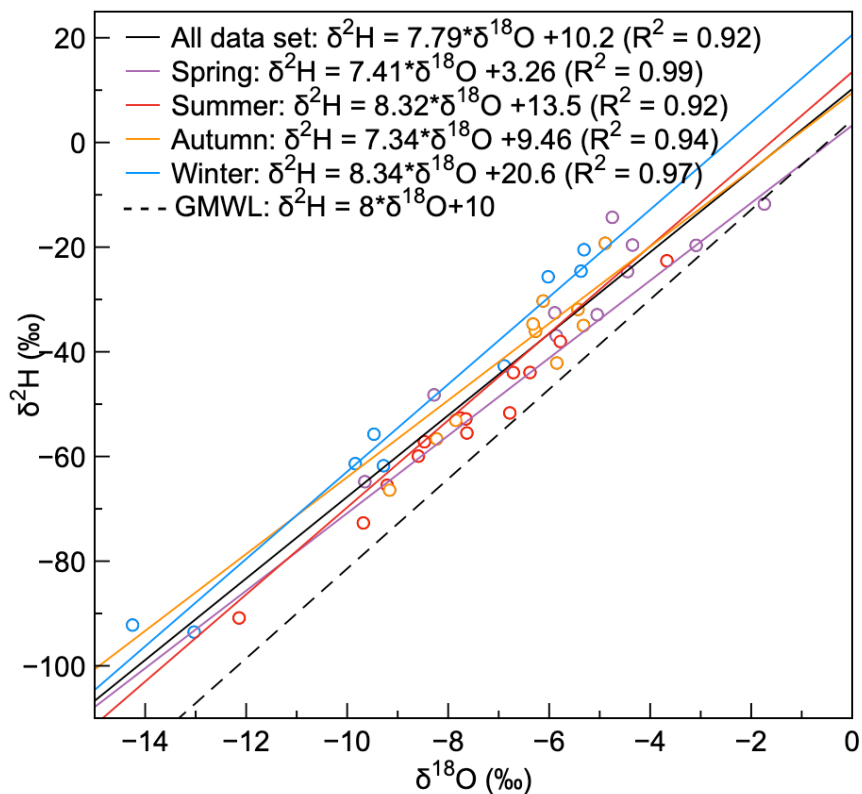


Figure 3: The monthly average values of the observed isotopic tracers. From top to bottom: $\delta^{17}\text{O}$, $\delta^{18}\text{O}$, $\delta^2\text{H}$, deuterium excess (d-excess), and ^{17}O -excess.



495 **Figure 4: The values of isotopic tracers by season, with regression lines for each. The black regression line represents the aggregated data for the entire year, which served as a baseline for seasonal variations. Red points and their regression line indicate the summer trend. Blue points with the corresponding regression line depict the winter values. The black dash line denotes the Global Meteoric Water Line (GMWL).**

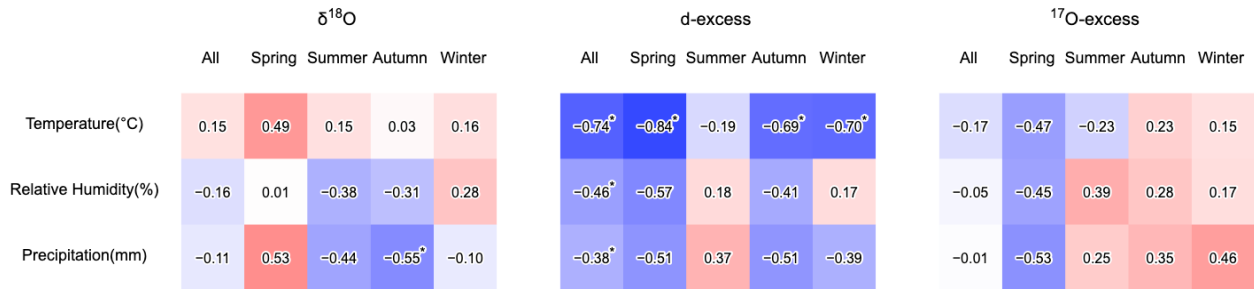
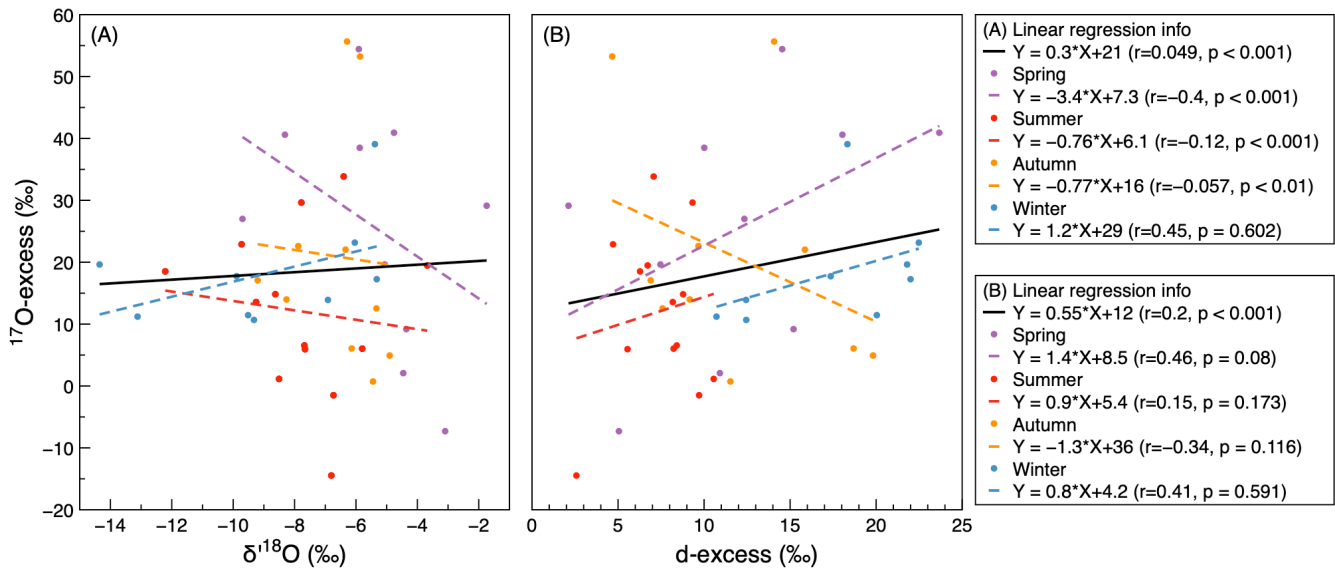


Figure 5: Correlations between precipitation-weighted mean monthly precipitation isotopes ($\delta^{18}\text{O}$, d-excess, and ^{17}O -excess) and the precipitation-weighted mean meteorological variables (air temperature, relative humidity) and total precipitation amount during the study period.



510 **Figure 6: The seasonal relationships between ^{17}O -excess and (A) $\delta^{18}\text{O}$ and (B) d-excess. Each marker represents a monthly weighted mean sample, color-coded by season (violet = spring; red = summer; orange = autumn; blue = winter). The regression line for each season is shown as a dashed line in the corresponding color, while the solid black lines represent the regression for the entire dataset. The regression equations and Pearson correlation coefficients (r) are listed in the legends.**

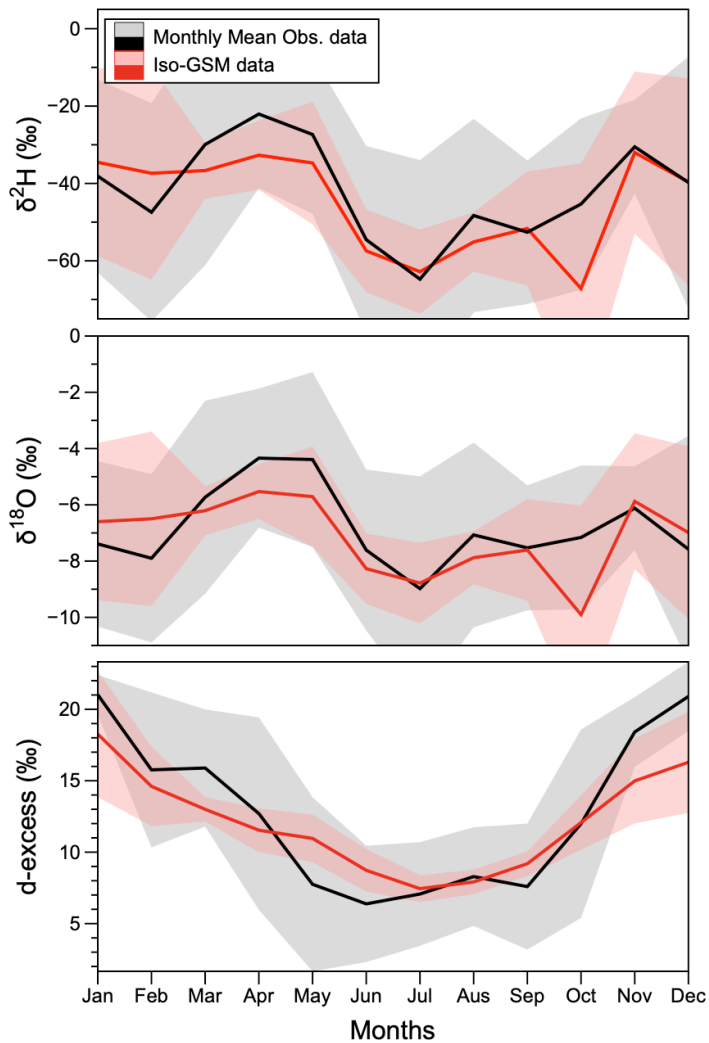


Figure 7: The monthly mean precipitation stable isotope values ($\delta^2\text{H}$, $\delta^{18}\text{O}$, and d-excess) from observations (black solid line with gray shading) and Isotope-enabled Global Spectral Model (Iso-GSM) outputs (red solid line with pink shading). The shaded areas represent the uncertainty range of the monthly mean (± 1 standard deviation), while the solid lines indicate the monthly average values.

515